Available online at www.sciencedirect.com
SCIENCE DIRECT®
Dyes and Pigments 60 (2004) 69–84
DYES and PIGMENTS
www.elsevier.com/locate/dyepig

Adsorption of anionic dyes in acid solutions using chemically cross-linked chitosan beads

Ming-Shen Chiou*, Pang-Yen Ho, Hsing-Ya Li

Department of Chemical Engineering, National United University, Miau Li 36003, Taiwan, ROC

Received 9 April 2003; received in revised form 7 June 2003; accepted 26 June 2003

Abstract

One kind of adsorbents with high adsorption capacity of anionic dyes was prepared using ionically and chemically cross-linked chitosan beads. A batch system was applied to study the adsorption of four reactive dyes (RB2, RR2, RY2, RY86), three acid dyes (AO12, AR14, AO7) and one direct dye (DR81) from aqueous solutions by the cross-linked chitosan beads. The adsorption capacities had very large values of 1911–2498 (g/kg) at pH 3–4, 30 °C, which were 3.4–15.0 and 2.7–27.4 times those of the commercial activated carbon and chitin, respectively. The Langmuir and Freundlich adsorption models were applied to describe the equilibrium isotherms. The Langmuir model agreed very well with experimental data ($R^2 > 0.9893$). The kinetics of adsorption, the ADMI color value and decolorization efficiency for different initial dye concentrations were evaluated by the pseudo first-order and second-order models. The data agreed very well with the pseudo second-order kinetic model. The adsorption capacity increased largely with decreasing solution pH and adsorbent dosage. The free energy changes ΔG^0 for adsorption of anionic dyes in acidic solutions at 30 °C were evaluated. The negative values of ΔG^0 indicate overall adsorption processes are spontaneous.

Keywords: Adsorption capacity; Anionic dyes; Cross-linked chitosan beads; Langmuir isotherm; Pseudo second-order model

1. Introduction

Various kinds of synthetic dyestuffs appear in the effluents of wastewater in some industries such as dyestuff, textiles, leather, paper, plastics, etc. Since a very small amount of dye in water is highly visible and can be toxic to creatures in water, the removal of color from process or waste effluents becomes environmentally important. Among several chemical and physical methods, the adsorption process is one of the effective techniques that have been successfully employed for color removal from wastewater. Many adsorbents have been tested on the possibility to lower dye concentrations from aqueous solutions, such as activated carbon [1,2], peat [3,4], chitin [5,6], silica [7] and others [8–16]. However, the amount (g) of dyes adsorbed on the above adsorbents (kg) are not very high, some have capacities between 200 and 600 g/kg and some even lower than 50 g/kg. To improve the efficiency of the adsorption processes, it is essential to develop the more effective and cheaper adsorbents with higher adsorption capacities.

Recently, chitosan has been observed for the high potentials of the adsorption of dyes [17,18], metal ions [19,34,35], proteins [20,36] and others

* Corresponding author. Tel.: +886-37-352840x62; fax: +886-37-332397.
E-mail address: chiou@mail.nuu.edu.tw (M.-S. Chiou).

0143-7208/$ - see front matter © 2003 Elsevier Ltd. All rights reserved.
doi:10.1016/S0143-7208(03)00140-2

[37,38]. The adsorption of reactive dyes in neutral solutions using chitosan showed large adsorption capacities of 1000–1100 g/kg [18]. Chitosan is the deacetylated form of chitin, which is a linear polymer of β-(1→4)acetyl-D-glucosamine. It contains high contents of amino functional groups, which might form electrostatic attraction between chitosan and solutes to adsorb the dyes [17,21] and proteins [20,36]. The binding ability of chitosan for metal ion is also mainly due to the chelating groups (the amino and hydroxyl groups) on the chitosan [28,34,39]. Other useful features of chitosan include its abundance, non-toxicity, hydrophilicity, biocompatibility, biodegradability, and anti-bacterial property [21].

There are at least two reasons to study the adsorption behavior of chitosan in acid aqueous solutions. First, the amino groups of chitosan are much easier to be cationized and they adsorb the dye anions strongly by electrostatic attraction [21]. Secondly, since acetic acid is often used as a stimulator in the dying process, in which the pH of the dye solution is normally adjusted to 3–4. However, chitosan formed gels below pH 5.5 and could not be evaluated. The acid effluent could severely limit the use of chitosan as an adsorbent in removing dyes and mental ions due to chitosan's dissolution tendency in the acid effluent.

Some cross-linking reagents [22,23] have been used to stabilize chitosan in acid solutions. Cross-linked chitosan is not only insoluble in acid solution but also has stronger mechanical properties. Yoshida et al. [17] used Denacol EX841 as a cross-linking reagent and obtained a high adsorption capacity (1200–1700 g/kg) of Acid Orange II (acid dye) on the cross-linked chitosan fibers in acid solutions of pH 3 and 4. Chiou and Li [24] cross-linked chitosan by epichlorohydrin (ECH) and obtained a high adsorption capacity (1600–1900 g/kg) of reactive dye (RR 189) on the cross-linked chitosan beads in acid aqueous solutions of pH 3. It appears technically feasible to remove acid and reactive dyes from acid aqueous solutions by cross-linked chitosan.

Although the cross-linked chitosan beads made in our previous work [24] were insoluble and had high adsorption capacity of RR 189 in acid aqueous solutions, they were soft beads and the mechanical property needed to be improved for practical applications. Moreover, we need to evaluate the adsorption behavior using more dyes. In this work, the solution of sodium tripolyphosphate (TPP) was used in the beads formation step to produce more rigid beads via its ionic cross-linking effect [25]. We investigated the equilibrium and kinetics of adsorption of eight anionic dyes in solutions of pH 3–8. The Langmuir and Freundlich equations were used to fit the equilibrium isotherms. The effects of pH and adsorbent dosage on adsorption capacity were studied. Uptakes of anionic dyes were also compared among cross-linked chitosan beads, commercial activated carbon and chitin at different pH. The dynamical behaviors of the adsorption, ADMI and decolorization efficiency were measured on the effect of initial dye concentration. The kinetics was determined quantitatively by the pseudo first-order and second-order models.

2. Materials and methods

2.1. Chemicals

Chitosan (α-type; extracted from snow crab shell, degree of deacetylation: 95.5%; average molecular weight: 200 kD) was supplied by OHKA Enterprises Co. and used as received. Commercial activated carbon (powder, extra pure) was supplied by Merck Co., Taiwan. Reagents: ECH (⩾98%) and TPP (⩾98%) were purchased from Fluka. The eight anionic dyes studied are the practical grade and used as received. Fig. 1 displays the structure of the eight anionic dyes and Table 1 displays their details.

2.2. Preparation of chitosan beads

The preparation of cross-linked chitosan beads is described in the followings [20,23,25–26]. Ten grams of chitosan were dissolved in 300 cm^3, 5 wt.% of acetic acid solution. The aqueous solution was diluted to 1.0 dm^3 by strong stirring over night, and then left to stay still for 6 h. Chitosan solution (10 cm^3) was dropped from the burette

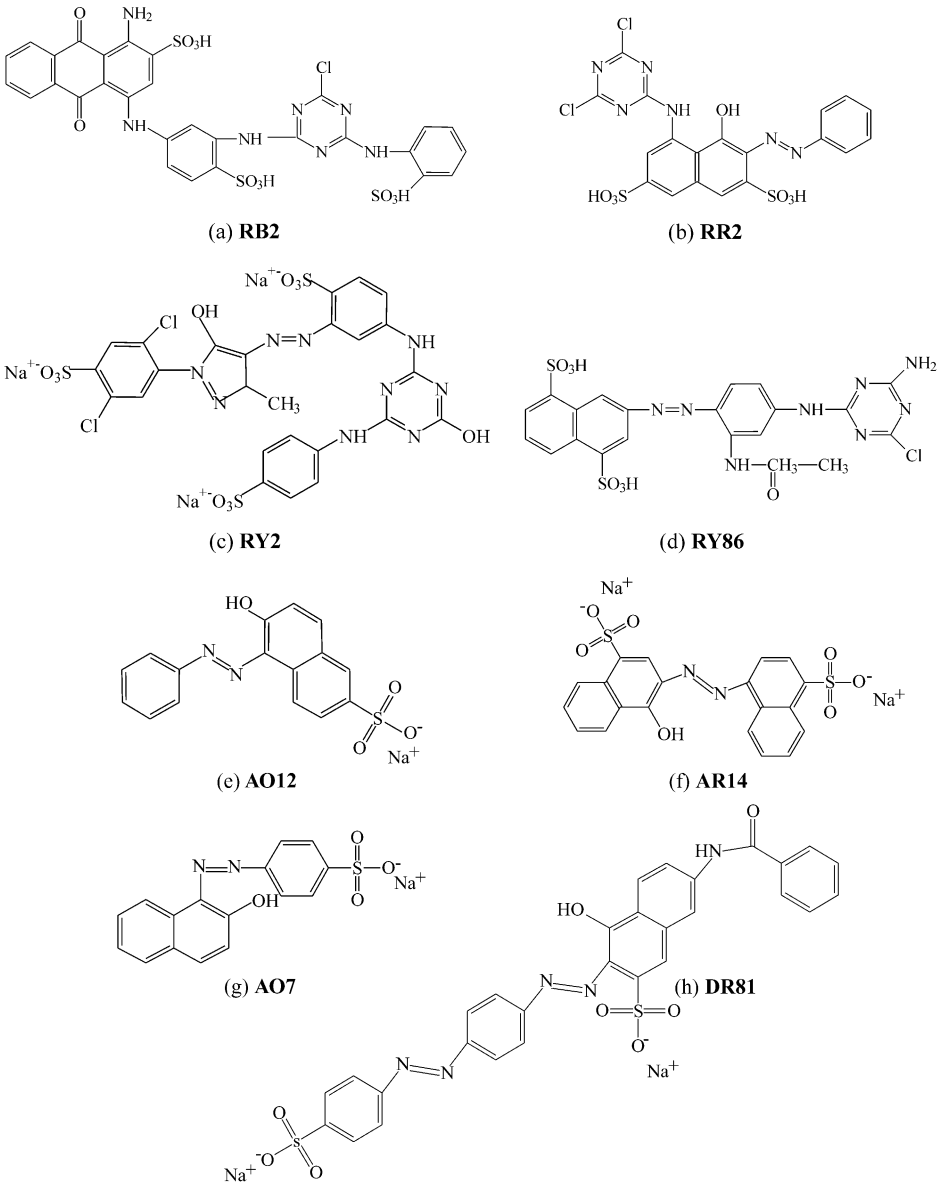

Fig. 1. The structures of anionic dyes.

into a 100-cm^3 aqueous solution of TPP (1 wt.%) and formed beads of diameters 2.3–2.5 mm. The ionically cross-linked chitosan beads were washed with deionized water, and stored in distilled water. The above ionically cross-linked chitosan beads, 50 cm^3 of 1 N sodium hydroxide solution, and chemical cross-linking reagent ECH were mixed and shaken for 6 h at 50 °C in a water bath (Deng Yng corp., Taiwan). The 0.5 of molar ratios of cross-linking reagents/chitosan was carried out in this work.

In our previous work [24], we studied the equilibrium adsorption of RR 189 at pH 3.0, 30 °C on the cross-linked chitosan beads for three different particle sizes (2.3–2.5, 2.5–2.7 and 3.5–3.8 mm). The adsorption capacity increased slightly with a

Table 1
Details of anionic dyes

Anionic dyes	λ_{max} (nm)	F.W. (g/mol)	Supplier
Reactive Blue 2 (RB2)	614	774.20	Sigma
Reactive Red 2 (RR2)	534	615.34	Aldrich
Reactive Yellow 2 (RY2)	402	872.97	Aldrich
Reactive Yellow 86 (RY86)	416	596.01	Sigma
Acid Orange 12 (AO12)	484	350.33	Aldrich
Acid Red 14 (AR14)	514	502.44	Aldrich
Acid Orange 7 (AO7)	484	350.33	Aldrich
Direct Red 81 (DR81)	508	675.61	Aldrich

decrease the diameter of the chitosan bead since the effective surface area is higher for the same mass of smaller particles. This might suggest that the adsorption took place mainly on the outer surfaces of the particles due to steric hindrance of large dye molecules. Thus, the beads of diameters 2.3–2.5 mm were used in this work to obtain a higher adsorption capacity. In our previous work [24], we also studied the equilibrium adsorption of RR 189 at pH 3.0, 30 °C on the cross-linked chitosan beads for four different cross-linking ratios (ECH/chitosn: 0.2, 0.5, 0.7 and 1.0). The uptakes in adsorption equilibrium are similar to each other for cross-linking ratio at 0.2, 0.5 and 0.7, and decreases slightly at ratio 1.0. Since the cross-linking ratio is only a minor factor in the adsorption of anionic dyes, 0.5 of molar ratio is carried out in this work for our convenience.

2.3. Batch equilibrium studies

Anionic dye solutions were prepared by dissolving dye in deionized water to the required concentrations. The pH of dye solutions was adjusted by buffer solutions of acetic acid/acetate. In experiments of equilibrium adsorption isotherm, the mixture of chitosan beads (containing 0.1 g dry basis of chitosan), dye solution (50 cm^3) and acetic acid buffer solution with desired pH value were shaken for 5 days using a bath to control the temperature at 30 ± 1 °C. In order to measure the dye concentration, the solutions were adjusted to pH 6.0 and analyzed by an UV/visible spectrometer (JASCO V-530) at wavelength corresponding to the maximum absorbance (λ_{max}) shown in Table 1. Eq. (1) was used to calculate the amount of adsorption at equilibrium q_e (g/kg):

$$q_e = (C_0 - C_e)V/W \quad (1)$$

where C_0 and C_e are the initial and equilibrium solution concentrations (g/m^3), respectively. V is volume of the solutions (m^3), and W is the weight of chitosan (dry basis, kg) used.

2.4. Batch kinetic studies

In experiments of batch kinetic adsorption, a mixture of the cross-linked chitosan beads (0.1 g dry basis of chitosan) and 50 cm^3 dye solution were shaken using a shaker with a water bath to control temperature. Every other period of time, 0.1 cm^3 of dye solution was taken out to dilute to 10 cm^3. Its concentration was determined using a UV/visible spectrometer after the pH was adjusted to 6.

The adsorption kinetics of a mixture of the four reactive dyes onto the cross-linked chitosan beads was studied by the ADMI (American Dye Manufacturers Institute) method. Two different initial concentrations were prepared. One has ADMI to be 43,500 c.u. with all the four reactive dyes at 450 g/m^3. The other one has ADMI to be 85,400 c.u. with RY2, RB2, RR2 and RY86 at 1362, 1298, 990 and 758 g/m^3, respectively. A mixture of the cross-linked chitosan beads (0.1 g dry basis of chitosan) and 50 cm^3 dye-mixture solution were shaken in a shaker at 30 °C. The pH of this solution was maintained at pH 3 by buffer solution. Every other period of time, 0.1 cm^3 of residual dye solution was taken out to dilute to a proper ADMI range (0–250 c.u.). The ADMI color values were determined using a spectrophotometer (HACH DR/4000) with a narrow (10 nm or less) spectral band and an effective operating range of 400–700 nm after the pH of diluted solution was adjusted to 7.6 [40].

3. Results and discussion

Comparing with our previous work [24], the chitosan beads made in this work were formed

faster. These beads are more rigid, due to the ionic attractions between $P_3O_{10}^{5-}$ (TPP) and the $-NH_3^+$ group of chitosan in acid solutions [25]. This improves the mechanical strength of the chitosan beads and the time required to form beads is also reduced. As the same in our previous work [24], we also select ECH as a chemical cross-linking reagent to cross-link the chitosan beads in alkaline condition. The ionic interaction between chitosan and TPP will disappear due to the deprotonation of adsorbent by 1 N sodium hydroxide before the chemical cross-linking reaction taking place in basic solution [25]. In our experiments, the chemically cross-linked chitosan beads are insoluble in acidic solutions of pH 3, while those not chemically cross-linked dissolve in acidic solutions below pH 5.5.

3.1. Adsorption isotherms

Fig. 2a and b show the adsorption isotherms of reactive, acid and direct dyes at 30 °C using the cross-linked chitosan beads. The equilibrium adsorption density q_e increased with increase in dye concentration. The shape of the isotherms looks rectangular because at low equilibrium dye concentrations C_e, the equilibrium adsorption densities q_e of the cross-linked chitosan beads reach almost the same q_e as those at high equilibrium dye concentrations. It indicates that the cross-linked chitosan beads have high adsorption density even at low equilibrium dye concentrations. The rectangular shape of the isotherms was also observed in Yoshida et al. [17].

The adsorption curves were applied to both the Langmuir and Freundlich equations. The widely used Langmuir isotherm has found successful application to many real sorption processes and is expressed as:

$$q_e = \frac{QbC_e}{1 + bC_e} \tag{2}$$

where Q (g/kg) is the maximum amount of the dye per unit weight of chitosan to form a complete monolayer coverage on the surface bound at high equilibrium dye concentration C_e, and b is the Langmuir constant related to the affinity of binding sites (m^3/g). Q represents a practical limiting adsorption capacity when the surface is fully covered with dye molecules and assists in the comparison of adsorption performance. Q and b are computed from the slopes and intercepts of the straight lines of plot of (C_e/q_e) vs. C_e.

The Freundlich isotherm is given as

$$q_e = Q_f C_e^{1/n} \tag{3}$$

where Q_f is roughly an indicator of the adsorption capacity and $(1/n)$ of the adsorption intensity [27]. Q_f and $1/n$ can be determined from the linear plot of $\ln(q_e)$ vs. $\ln(C_e)$.

Parameters of the Langmuir and Freundlich isotherms were computed in Table 2. The Langmuir isotherm fits quite well with the experimental data (correlation coefficient $R^2 > 0.9952$ for reactive dyes, > 0.9893 for acid dyes, $= 0.9985$ for DR81), whereas the low correlation coefficients ($R^2 < 0.7528$ for reactive dyes, < 0.6670 for acid dyes, $= 0.2253$ for DR81) show poor agreement of Freundlich isotherm with the experimental data. Table 2 indicates that the computed maximum monolayer capacity Q on the cross-linked chitosan beads has large value, ranging from 1911 to 2498 g/kg for reactive dyes, 1940 to 1954 g/kg for acid dyes, and equal to 2383 g/kg for direct dye. Table 3 lists the comparison of maximum monolayer adsorption capacity of some dyes on various adsorbents. Compared with some data in the literature, Table 3 shows that the cross-linked chitosan beads studied in this work have very large adsorption capacity.

3.2. Effect of initial dye concentration

Fig. 3a and b show that the effect of initial dye concentration on the adsorption kinetics of the cross-linked chitosan at 30 °C with respect to the anionic dyes. An increase in initial dye concentration leads to an increase in the adsorption capacity of dye on chitosan. According to Fig. 3a, the adsorption capacity of RB2 for 6 h with initial dye concentrations at 5286, 3962, 3592 and 3086 g/m^3 are 136, 91, 71 and 49% greater than that at 2089 g/m^3, respectively. This indicates that the initial dye concentrations play an important role in the adsorption capacities of RB2 on the cross-linked

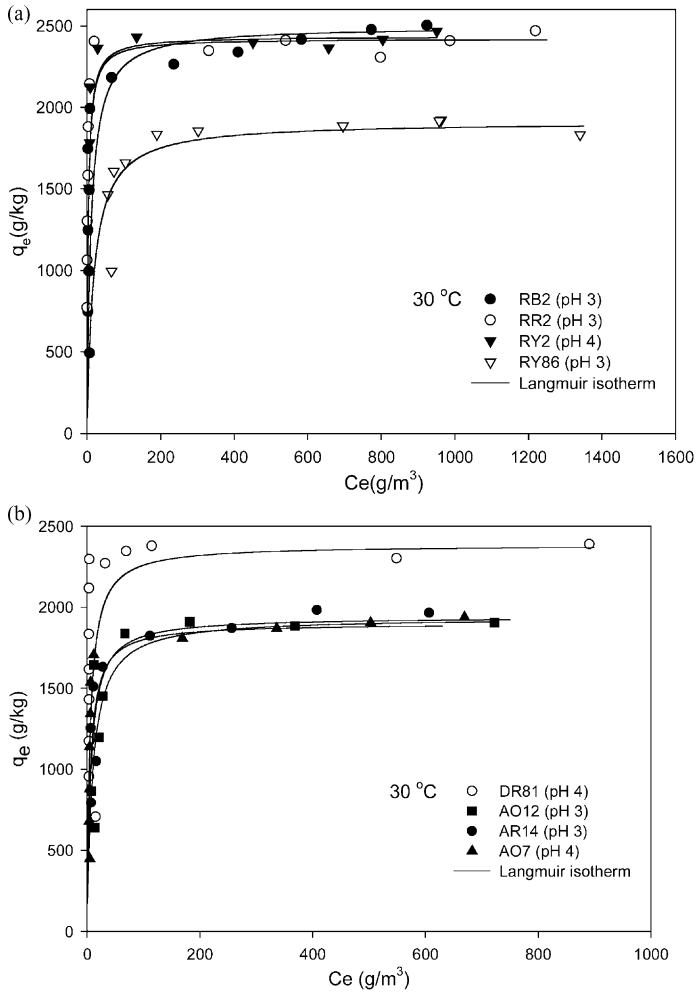

Fig. 2. Equilibrium adsorption isotherm of (a) reactive dyes and (b) acid and direct dyes on cross-linked chitosan beads.

chitosan beads. The similar effect is also observed by the other anionic dye [24].

In order to investigate the mechanism of adsorption, the pseudo first-order and the pseudo second-order adsorption models were used to test dynamical experimental data. The first-order rate expression of Lagergren is given as:

$$\log(q_e - q) = \log q_e - \frac{k_1}{2.303} t \tag{4}$$

where q_e and q are the amounts of dye adsorbed on adsorbent at equilibrium and at time t, respectively (g/kg) and k_1 is the rate constant of first-order adsorption (min^{-1}). The slopes and intercepts of plots of $\log(q_e - q)$ vs. t were used to determine the first-order rate constant k_1. In many cases the first-order equation of Lagergren does not fit well to the whole range of contact time and is generally applicable over the initial stage of the adsorption processes [29].

The second-order kinetic model [30] is expressed as

$$\frac{t}{q} = \frac{1}{k_2 q_e^2} + \frac{t}{q_e} \tag{5}$$

where k_2 (kg g^{-1} min^{-1}) is the rate constant of second-order adsorption. The slopes and intercepts

Table 2
Langmuir and Freundlich isotherm constants for anionic dyes (pH 3, 30 °C)

	Langmuir			Freundlich		
	Q (g/kg)	b (m^3/g)	R^2	Q_f	n	R^2
Reactive dye						
RB2	2498	0.091	0.9990	907	6.38	0.5116
RR2	2422	0.302	0.9990	1320	9.82	0.7528
RY2 (pH4)	2436	0.302	0.9952	1646	15.95	0.6273
RY86	1911	0.055	0.9977	884	8.75	0.4899
Acid dye						
AO12	1954	0.092	0.9994	736	6.27	0.5433
AR14	1940	0.138	0.9893	842	6.90	0.6670
AO7 (pH4)	1940	0.152	0.9995	756	6.31	0.4961
Direct dye						
DR81 (pH4)	2383	0.182	0.9985	1316	10.78	0.2253

of plots of t/q vs. t were used to calculate the second-order rate constant k_2 and q_e. It is more likely to predict the behavior over the whole range of adsorption and is in agreement with the chemisorption mechanism being the rate-controlling step [29,30].

Table 4 lists the results of rate constant studies for different initial dye concentrations by the pseudo first-order and second-order models. The correlation coefficient R^2 for the pseudo second-order adsorption model has extreme high value (> 0.9969 for reactive dyes, > 0.9983 for acid dyes), and its calculated equilibrium adsorption capacities $q_{e,\mathrm{cal}}$ is consistent with the experimental data. These suggest that the pseudo second-order adsorption mechanism is predominant and that the overall rate of the dye adsorption process appears to be controlled by the chemisorption process [29,30]. The similar phenomena have also been observed in biosorption of dye RB2, RY2, and Remazol Black B on biomass [13,31]. For the pseudo second-order model in Table 4, in general, the rate constant decreases with an increasing of initial dye concentration.

According to the pseudo-second order model, the adsorption rate $\mathrm{d}q/\mathrm{d}t$ is proportional to the second order of $(q_e - q)$. Since the cross-linked chitosan beads in our experiments have very high equilibrium adsorption capacities q_e, the adsorption rates become very fast and the equilibrium times are short. Take dye RB2 in Fig. 3a for an example. The adsorption density q_t at 2 h for all the initial concentrations reaches over 94% of the calculated equilibrium adsorption capacity $q_{e,\mathrm{cal}}$ in Table 4. Such short equilibrium times coupled with high adsorption capacity indicate a high degree of affinity between the anionic dyes and the cross-linked chitosan beads [31].

The adsorption kinetics of a mixture of the four reactive dyes onto the cross-linked chitosan beads at pH 3, 30 °C is shown in Fig. 4. It indicates that the ADMI of the mixture of the dye solution decreases with contact time. The equilibrium time is about 40 and 100 min for initial concentration of 43,500 and 85,400 ADMI, respectively. The decolorization efficiency of the two initial concentrations increases with contact time. The decolorization efficiency of the lower initial concentration reaches almost 100%, while that of the higher concentration approaches saturation.

Similar to the adsorption kinetics of a single dye discussed above, the kinetics of the decolorization efficiency of the dye mixture can be described by the pseudo first-order and second-order rate model in Eqs. (6) and (7), respectively.

$$\log(d_e - d) = \log d_e - \frac{k_{d1}}{2.303} t \tag{6}$$

$$\frac{t}{\mathrm{d}} = \frac{1}{k_{d2} d_e^2} + \frac{t}{d_e} \tag{7}$$

where d_e and d are the decolorization efficiency at equilibrium and at time t, respectively (%); k_{d1}, k_{d2} are, respectively, the rate constants of the first-order

Table 3
Comparison of the maximum monolayer adsorption capacities of some dyes on various adsorbents

Dyes	Adsorbent	Maximum monolayer adsorption capacities (g/kg)	Reference
RB2, RR2	Chitosan bead (cross-linked, TPP)	2498, 2422	This work
RO14, RY86	Chitosan bead (cross-linked, TPP)	2171, 1911	This work
AO12, AR14, AO7	Chitosan bead (cross-linked, TPP)	1940–1954	This work
DR81	Chitosan bead (cross-linked, TPP)	2383	This work
Deorlene Yellow	Activated carbon	~200	[1]
Telon Blue	Activated carbon	~160	[1]
AB 25	Carbon, peat, alumina	83–99	[2]
BB 3	Activated carbon, fuller's earth	448–560	[2]
BR 22	Activated carbon, fuller's earth	460–520	[2]
BB 69	Peat	184–233	[4]
AB 25	Peat	5–9	[4]
Mordant Yellow 5	Chitin	52	[5]
AB 25	Chitin	183	[5]
AB 158	Chitin	216	[5]
Direct Red 84	Chitin	44	[5]
RR 222	Chitosan (non-cross-linked)	299–380	[6]
RR 222	Chitin	~100	[6]
RR 222	Activated carbon	~50	[6]
RB 222	Chitosan (non-cross-linked)	54–87	[6]
RY 145	Chitosan (non-cross-linked)	117–179	[6]
Astrazone Blue	Silica	~25	[7]
Astrazon Blue	Maize cob	160	[8]
Erionyl Red	Maize cob	48	[8]
RY 2	Bacteria	52–124	[9]
RB 2	Rice husk	130	[10]
Acid Brilliant Blue	Banana pith	4–5	[11]
Acid Orange 10	Activated carbon	2–6	[12]
RY 2	Activated sludge	333	[13]
RB 2	Activated sludge	250	[13]
Congo Red	Activated carbon (coir pith)	7	[15]
MO, MB, RB	Banana and orange peel	14–21	[16]
CR, MV, AB	Banana and orange peel	6–18	[16]
Acid Orange II	Chitosan fiber (cross-linked)	1226–1678	[17]
RR 222	Chitosan (non-cross-linked)	1026–1106	[18]
RR 189	Chitosan bead (cross-linked, NaOH)	1642–1936	[24]
RR 189	Chitosan bead (non-cross-linked, NaOH)	1189	[24]
Remazol Black B	Fungus	286–588	[31]
Acid Violet 17	Orange peel	20	[32]
AB 29	Peat, fly ash	14–15	[33]
BB 29	Peat, fly ash	54–46	[33]
Disperse Red 1	Peat, bentonite, slag, fly ash	23–50	[33]

and second-order adsorption (min^{-1}). Table 5 lists the results of rate constant studies for different initial dye concentrations of the reactive dye mixture by the first-order and second-order models. The correlation coefficient R^2 for the pseudo second-order adsorption model has high value (>0.9981), and its calculated equilibrium decolorization efficiency $d_{e,cal}$ is consistent with the experimental data. This result is similar to that of a single dye discussed above.

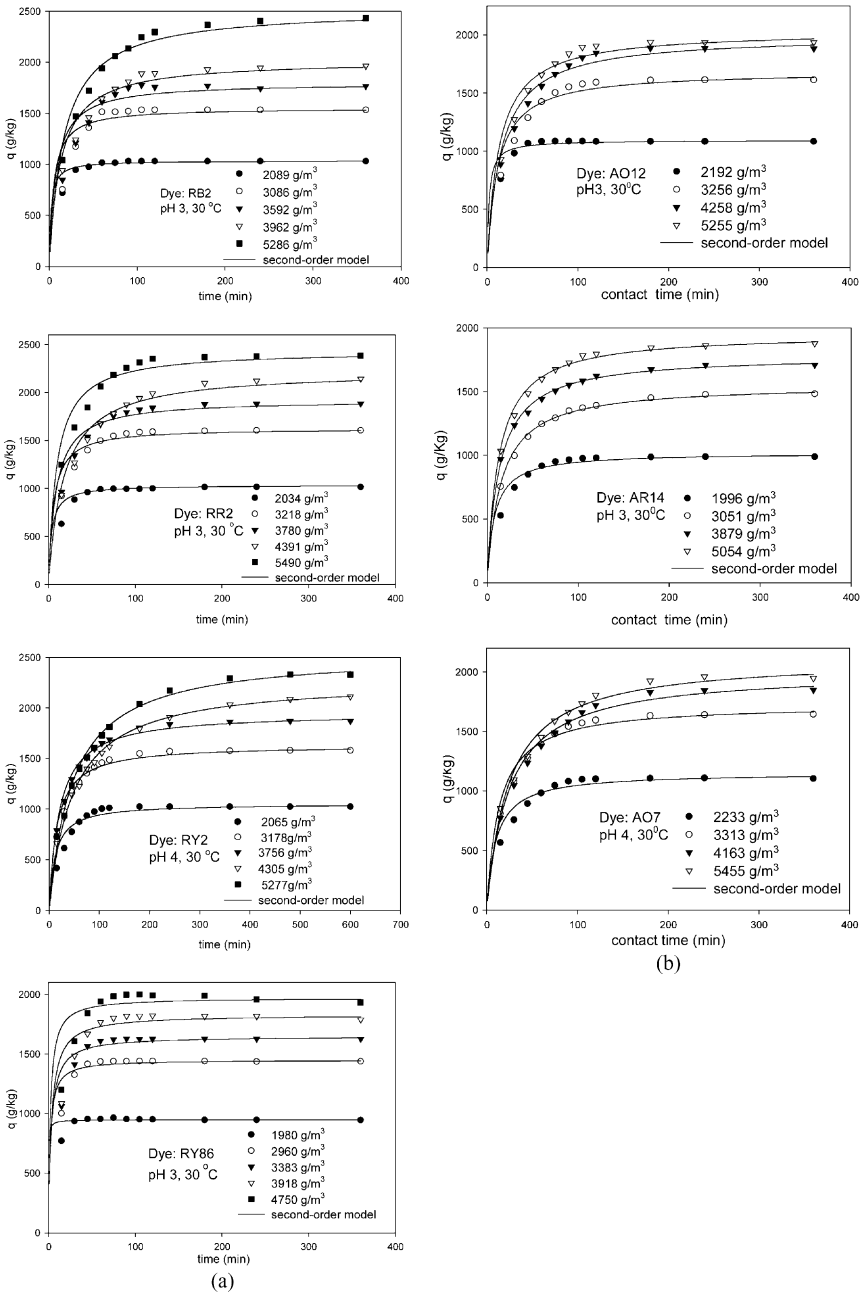

Fig. 3. Adsorption kinetics of (a) reactive dyes, (b) acid dyes on cross-linked chitosan beads at different initial dye concentrations.

3.3. *Effect of pH*

Fig. 5a and b shows the effect of pH on adsorption of the anionic dyes onto the cross-linked chitosan beads (CLCB), the commercial activated carbon (CAC) and chitin at 30 °C. For the commercial activated carbon and chitin, the adsorption capacities of the anionic dyes are affected very slightly by the pH, except for RR2 adsorbed by chitin. However, the pH affects significantly the

Table 4
Comparison of the first-order and second-order adsorption rate constants, calculated q_e and experimental q_t values for different initial dye concentrations (pH 3, 30 °C, $t = 6$ h)

Dye	Initial dye conc. (g/m^3)	q_t (g/kg)	First-order kinetic model			Second-order kinetic model		
			k_1 (min^{-1})	$q_{e,cal}$ (g/kg)	R^2	k_2 (kg g^{-1} min^{-1})	$q_{e,cal}$	R^2
Reactive dye								
RB 2	2089	1031	0.0506	507	0.9229	4.76×10^{-4}	1037	0.9999
	3086	1534	0.0596	1812	0.9172	1.32×10^{-4}	1553	0.9995
	3592	1766	0.0521	2748	0.9418	7.29×10^{-5}	1799	0.9993
	3962	1965	0.0185	966	0.9377	3.94×10^{-5}	2021	0.9995
	5286	2434	0.0171	1428	0.9783	2.38×10^{-5}	2524	0.9995
RR 2	2034	1015	0.0280	273	0.7955	2.80×10^{-4}	1024	0.9999
	3218	1605	0.0409	1281	0.9996	1.10×10^{-4}	1627	0.9998
	3780	1883	0.0315	1430	0.9986	5.98×10^{-5}	1924	0.9997
	4391	2142	0.0186	1459	0.9956	2.54×10^{-5}	2228	0.9996
	5490	2386	0.0231	1205	0.9535	4.35×10^{-5}	2436	0.9996
RY 2 (pH 4)	2065	1024	0.0380	1292	0.9885	8.05×10^{-5}	1053	0.9989
	3178	1576	0.0159	772	0.9702	4.05×10^{-5}	1633	0.9996
	3757	1864	0.0151	1141	0.9966	2.53×10^{-5}	1950	0.9996
	4305	2032	0.0082	1431	0.9964	9.43×10^{-6}	2280	0.9996
	5277	2294	0.0107	1868	0.9978	8.35×10^{-6}	2545	0.9991
RY 86	1980	946	0.0636	319	0.8489	4.76×10^{-3}	948	0.9999
	2963	1437	0.0864	1283	0.9592	3.62×10^{-4}	1450	0.9997
	3383	1626	0.0812	2221	0.9974	2.03×10^{-4}	1648	0.9995
	3918	1787	0.0648	2320	0.9839	1.62×10^{-4}	1828	0.9988
	4750	1932	0.0827	4676	0.9394	2.38×10^{-4}	1971	0.9985
Acid dye								
AO12	2192	1084	0.1077	2004	0.9886	4.29×10^{-4}	1095	0.9997
	3256	1614	0.0305	1109	0.9878	5.22×10^{-5}	1687	0.9986
	4258	1883	0.0303	1808	0.9803	3.27×10^{-5}	1994	0.9984
	5255	1938	0.0334	1907	0.9869	3.80×10^{-5}	2037	0.9985
AR14	1996	989	0.0336	586	0.9832	1.25×10^{-4}	1020	0.9991
	3051	1481	0.0203	904	0.9894	4.36×10^{-5}	1555	0.9998
	3879	1710	0.0239	1233	0.9444	4.21×10^{-5}	1784	0.9998
	5054	1878	0.0174	819	0.7925	4.04×10^{-5}	1955	0.9998
AO 7 (pH 4)	2233	1105	0.0331	910	0.9974	8.64×10^{-5}	1152	0.9984
	3313	1645	0.0232	990	0.9898	4.23×10^{-5}	1728	0.9991
	4163	1847	0.0198	1497	0.9955	2.05×10^{-5}	2006	0.9985
	5455	1946	0.0184	1500	0.9978	1.95×10^{-5}	2115	0.9983

adsorption capacities of the anionic dyes onto the cross-linked chitosan beads. In general, the uptakes are much higher in acidic solutions than those in neutral and alkaline conditions. The maximum values of the adsorption capacity ratio between acidic and alkaline conditions reach 2.7, 1.5, 2.0, 1.2, 19.1, 6.1, 65.6 and 4.6 for RB2 (pH4/pH8), RR2 (pH3/pH8), RY2 (pH4/pH7), RY86 (pH3/pH8), AO12 (pH3/pH7), AR14 (pH3/pH8), AO7 (pH3/pH8) and DR81 (pH3/pH8), respectively. The adsorption capacities of the anionic dyes onto the cross-linked chitosan beads are much higher than those of the commercial activated carbons and chitin at the same pH. Cross-linked

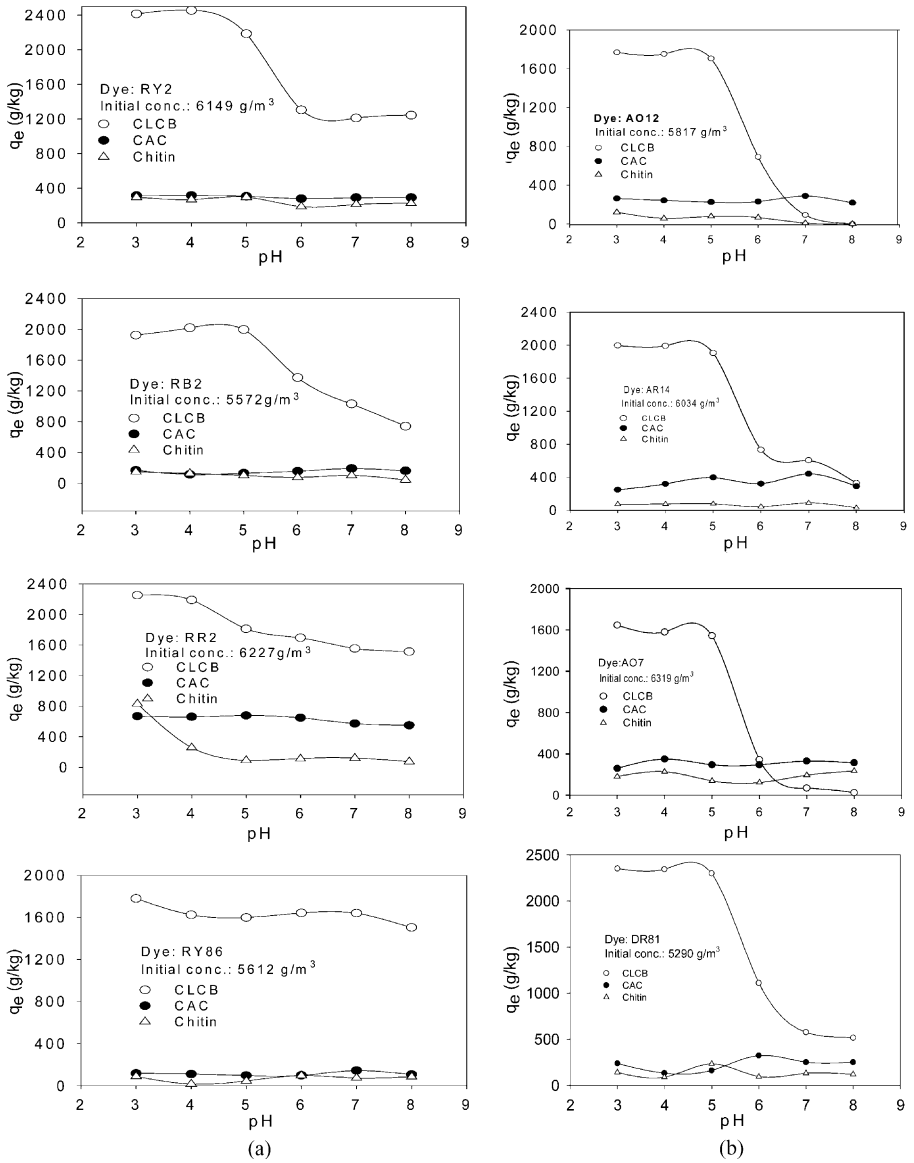

Fig. 4. The kinetics of ADMI and decolorization efficiency of a mixture of reactive dyes (RB2, RR2, RY2, RY86) for different initial concentrations at pH 3, 30 °C.

chitosan appears to be much more efficient than commercial activated carbon and chitin for adsorption of colors removal of anionic dyes. The ratio of the adsorption capacities at pH 3 between cross-linked chitosan beads and activated carbon are 11.5, 3.4, 7.7, 15.0, 6.7, 8.1, 6.3 and 9.9 for RB2, RR2, RY2, RY86, AO12, AR14, AO7 and DR81, respectively. The ratio of the adsorption capacities at pH 3 between cross-linked chitosan beads and chitin are 13.0, 2.7, 8.1, 19.9, 14.5, 27.4, 9.1 and 16.7 for RB2, RR2, RY2, RY86, AO12, AR14, AO7 and DR81, respectively.

According to Yoshida [17] and Kumar [21], at lower pH more protons will be available to protonate amine groups of chitosan molecules to form groups $-NH_3^+$, thereby increasing electrostatic

Table 5
Comparison of the first-order and second-order decolorization rate constants, calculated $d_{e,cal}$ and experimental d_t values for two different initial concentrations of the reactive dye mixture (pH 3, 30 °C)

		First-order kinetic model			Second-order kinetic model		
Initial conc. (ADMI)	d_t (%)	k_{d1} (min^{-1})	$d_{e,cal}$ (%)	R^2	k_{d2} (min^{-1})	$d_{e,cal}$ (%)	R^2
85,400	86.53(6 h)	2.68×10^{-2}	41.89	0.9452	1.18×10^{-3}	89.60	0.9993
43,500	98.23(3 h)	2.29×10^{-2}	16.31	0.6722	1.95×10^{-3}	101.37	0.9981

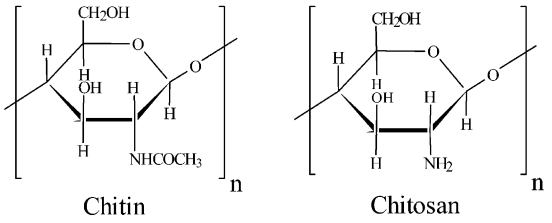

Fig. 5. The effect of pH on the adsorption capacity of (a) reactive dyes and (b) acid and direct dyes onto cross-linked chitosan beads (CLCB), commercial activated carbon (CAC) and chitin at 30 °C.

attractions between negatively charged dye anions and positively charged adsorption sites and causing an increase in dye adsorption. This explanation agrees with our data on pH effect. It can be seen that the pH of aqueous solution plays an important role in the adsorption of reactive dyes onto chitosan. The similar pH effects were also observed by the adsorption of acid dye on cross-linked chitosan fibers [17] and the adsorption of RR 189 (reactive dye) on cross-linked chitosan beads [24].

Besides the pH dependence showing the evidence of the electrostatic interaction, the adsorption behavior of chitosan and chitin also emphasize this evidence. Fig. 5a and b show that the adsorption capacities of chitosan are much higher than those of chitin for anionic dyes. This comes from the difference of the structure between chitosan and chitin, showing in Fig. 6. The chitosan contains amine group, –NH_2, which is easily protonated to form $-NH_3^+$ in acidic solutions. The high adsorption capacity is due to the strong electrostatic interaction between the $-NH_3^+$ of chitosan and dye anions. The chitin contains amide group, –CO–NH–, which cannot be easily protonated in acidic solutions. Since the electron withdrawal by carbonyl group makes the nitrogen of the amide group a much poorer source of electrons than that of the amine group. Electrons are less available for sharing with a hydrogen ion, and therefore amide is a much weaker base than amine. The low adsorption capacity of chitin is due to the lack of electrostatic interaction between chitin and dye anions. Fig. 6 also indicates that the major adsorption site is neither –OH nor –CH_2OH, for which both chitin and chitosan have the same amount. The adsorption capacity of a cationic dye (Basic violet 3, C.I. 42555, F.W. 407.985) onto the chemical cross-linked chitosan beads was also studied. Almost no adsorption was measured at pH 3, 30 °C. The electrostatic interaction can also be applied to explain the huge difference of adsorption capacity between anionic dyes and cationic dyes.

3.4. Effect of adsorbent dosage

Fig. 7 shows the adsorption density of reactive dyes onto the cross-linked chitosan beads for different adsorbent doses (20–100 mg/50 ml) at pH 3, 30 °C, 48 h. The ratios of the adsorption density (20 mg/100 mg) are 2.9, 3.9 and 3.6 for RB2, RR2 and RY86, respectively. The adsorption density increases significantly with decrease in the adsorbent dosage. This result is caused by that the smaller amount of adsorbent implies the higher amount of the dye contact with per unit weight of the adsorbent. The adsorption capacities are much improved by minimum effective substrate. The similar phenomena were also observed by the adsorption of textile dyes onto wheat straw and apple pomace [14].

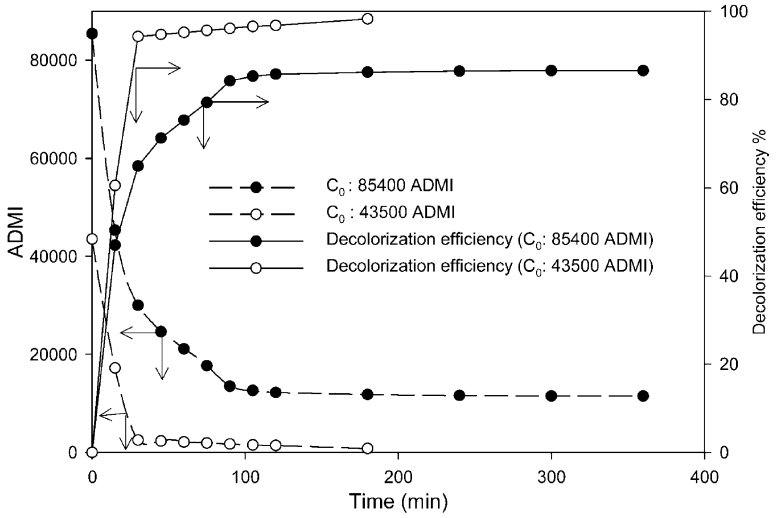

Fig. 6. The structural diagram of chitin and chitosan.

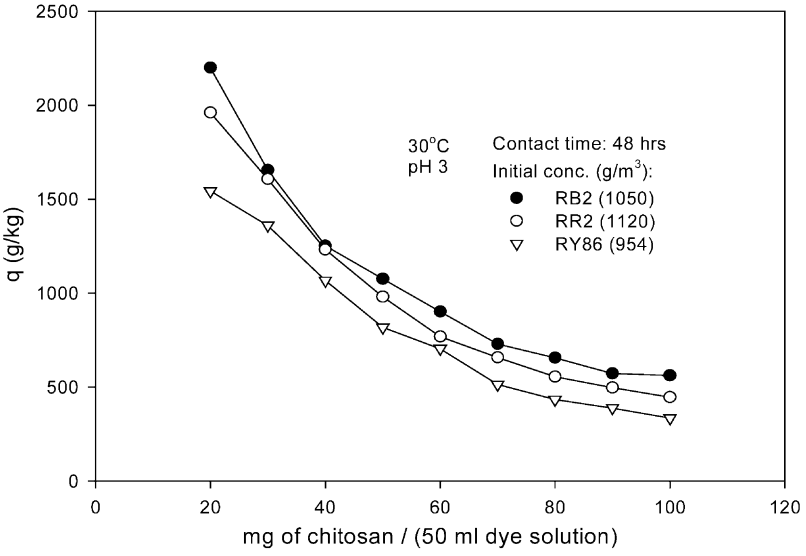

Fig. 7. The effect of adsorbent dosage on the adsorption capacity of reactive dyes onto cross-linked chitosan beads.

3.5. Changes of free energy

The free energy changes ΔG^0 for adsorption of anionic dyes in acidic solutions at 30 °C were evaluated using the following equations [31]:

$$K_C = \frac{C_{Ae}}{C_e} \tag{8}$$

$$\Delta G^0 = -RT \ln K_C \tag{9}$$

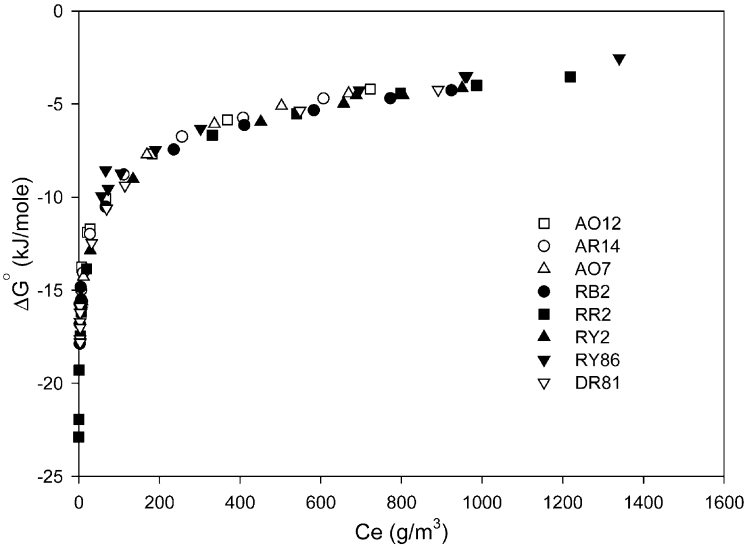

Fig. 8. Change in free energy with respect to different equilibrium concentrations for the adsorption of anionic dyes on cross-linked chitosan beads at 30 °C.

where K_C is the equilibrium constant, C_{Ae} is the amount of dye (g) adsorbed on the adsorbent per m^3 of the solution at equilibrium, C_e is the equilibrium concentration (g/m^3) of the dye in the solution, T is the solution temperature of Kelvin (K) and R is the gas constant. The isotherm data in Fig. 2a and b were applied to compute the changes of free energy. Fig. 8 shows the plots of ΔG^0 vs. C_e for adsorption of anionic dyes. The negative values of ΔG^0 indicate overall adsorption processes are spontaneous. At low equilibrium concentration C_e of the dye solutions in Fig. 8, the more negative values of ΔG^0 imply the greater the driving force of the adsorption process than that at higher C_e.

4. Conclusions

This study investigates the equilibrium and the dynamics of the adsorption of eight anionic dyes on the chemically cross-linked chitosan beads. The cross-linked chitosan beads had very high adsorption capacities to remove the anionic dyes, whose maximum monolayer adsorption capacity ranges from 1911 to 2498 (g/kg) at 30 °C. The adsorption capacities are affected significantly by the dye initial concentration, pH and adsorbent dosage. The uptake increases with increase in dye initial concentration, with decreases in pH and adsorbent dosage. To compare with commercial activated carbon, the cross-linked chitosan exhibits excellent performance for adsorption of anionic dyes. The adsorption capacities of the cross-linked chitosan beads are much higher than those of chitin for anionic dyes. It shows that the major adsorption site of chitosan is an amine group, $-NH_2$, which is easily protonated to form $-NH_3^+$ in acidic solutions. The strong electrostatic interaction between the $-NH_3^+$ of chitosan and dye anions can be used to explain the high adsorption capacity of anionic dyes onto chemically cross-linked chitosan beads. The Langmuir equation agrees very well with the equilibrium isotherm. The pseudo second-order kinetic model fits very well with the dynamical adsorption behavior, ADMI, and decolorization efficiency for different initial dye concentrations.

Acknowledgements

The partial financial support of this work by the Lien Ho Industry, Commerce, and Education Foundation, ROC, under the Grant No. 91-0-B1-E3-01 is gratefully acknowledged.

References

[1] McKay G. The adsorption of dyestuffs from aqueous solution using activated carbon: analytical solution for batch adsorption based on external mass transfer and pore diffusion. Chem Eng J 1983;27:187–96.

[2] Allen SJ. Types of adsorbent materials. In: McKay G, editor. Use of adsorbents for the removal of pollutants from wastewaters. Boca Raton (USA): CRC; 1996. p. 59–97.

[3] Ramakrishna KR, Viraraghavan T. Dye removal using low cost adsorbents. Water Sci Technol 1997;36:189–96.

[4] Ho YS, McKay G. Sorption of dye from aqueous solution by peat. Chem Eng J 1998;70:115–24.

[5] McKay G, Blair HS, Gardner JR. Rate studies for the adsorption of dyestuffs on chitin. J Colloid Interface Sci 1983;95:108–19.

[6] Juang RS, Tseng RL, Wu FC, Lee SH. Adsorption behavior of reactive dyes from aqueous solutions on chitosan. J Chem Technol Biotechnol 1997;70:391–9.

[7] McKay G. Analytical solution using a pore diffusion model for a pseudoirreversible isotherm for the adsorption of basic dye on silica. AIChE J 1984;30:692–7.

[8] El-Geundi MS. Color removal from textile effluents by adsorption techniques. Water Res 1991;25:271–3.

[9] Hu TL. Removal of reactive dyes from aqueous solution by different bacterial genera. Water Sci Technol 1996;34: 89–95.

[10] Low KS, Lee CK. Quaternized rice husk as sorbent for reactive dyes. Bioresource Technol 1997;61:121–5.

[11] Namasivayam C, Prabha D, Kumutha M. Removal of direct red and acid brilliant blue by adsorption on to banana pith. Bioresource Technol 1998;64:77–9.

[12] Tsai WT, Chang CY, Lin MC, Chien SF, Sun HF, Hsieh MF. Adsorption of acid dye onto activated carbon prepared from agricultural waste bagasse by $ZnCl_2$ activation. Chemosphere 2001;45:51–8.

[13] Aksu Z. Biosorption of reactive dyes by dried activated sludge: equilibrium and kinetic modelling. Biochem Eng J 2001;7:79–84.

[14] Robinson T, Chandran P, Nigam P. Removal of dyes from a synthetic textile dye effluent by biosorption on apple pomace and wheat straw. Water Res 2002;36:2824–30.

[15] Namasivayam C, Kavitha D. Removal of Congo Red from water by adsorption onto activated carbon prepared from coir pith, an agricultural solid waste. Dyes and Pigments 2002;54:47–58.

[16] Annadurai G, Juang RS, Lee DJ. Use of cellulose-based wastes for adsorption of dyes from aqueous solutions. J Hazard Mater 2002;B92:263–74.

[17] Yoshida H, Okamoto A, Kataoka T. Adsorption of acid dye on cross-linked chitosan fibers: equilibria. Chem Eng Sci 1993;48:2267–72.

[18] Wu FC, Tseng RL, Juang RS. Comparative adsorption of metal and dye on flake- and bead-types of chitosans prepared from fishery wastes. J Hazard Mater 2000;B73:63–75.

[19] Guibal E, Milot C, Tobin JM. Metal-anion sorption by chitosan beads: equilibrium and kinetic studies. Ind Eng Chem Res 1998;37:1454–63.

[20] Zeng XF, Ruckenstein E. Cross-linked macroporous chitosan anion-exchange membranes for protein separations. J Membr Sci 1998;148:195–205.

[21] Kumar MNVR. A review of chitin and chitosan applications. React Funct Polym 2000;46:1–27.

[22] Wei YC, Hudson SM, Mayer JM, Kaplan DL. The crosslinking of chitosan fibers. J Polym Sci: Polym Chem 1992;30:2187–93.

[23] Zeng XF, Ruckenstein E. Control of pore sizes in macroporous chitosan and chitin membranes. Ind Eng Chem Res 1996;35:4169–75.

[24] Chiou MS, Li HY. Equilibrium and kinetic modeling of adsorption of reactive dye on cross-linked chitosan beads. J Hazard Mater 2002;B93:248–63.

[25] Mi FL, Shyu SS, Lee ST, Wong TB. Kinetic study of chitosan-tripolyphosphate complex reaction and acid-resistive properties of the chitosan- tripolyphosphate gel beads prepared by in-liquid curing method. J Polym Sci: Polym Phys 1999;37:1551–64.

[26] Chiou MS, Li HY. Adsorption behavior of reactive dye in aqueous solution on chemical cross-linked chitosan beads. Chemosphere 2003;50:1095–105.

[27] McKay G, Blair HS, Gardner JR. Adsorption of dyes on chitin—I: equilibrium studies. J App Poly Sci 1982;27: 3043–57.

[28] Chu KH. Removal of copper from aqueous solution by chitosan in prawn shell: adsorption equilibrium and kinetics. J Hazard Mater 2002;90:77–95.

[29] McKay G, Ho YS. The sorption of lead (II) on peat. Water Res 1999;33:578–84.

[30] McKay G, Ho YS. Pseudo-second order model for sorption processes. Process Biochem 1999;34:451–65.

[31] Aksu Z, Tezer S. Equilibrium and kinetic modelling of biosorption of remazol black B by rhizopus arrhizus in a batch system: effect of temperature. Process Biochem 2000;36:431–9.

[32] Sivaraj R, Namasivayam C, Kadirvelu K. Orange peel as an adsorbent in the removal of acid violet 17 (acid dye) from aqueous solutions. Waste Management 2001;21:105–10.

[33] Ramakrishna KR, Viraraghavan T. Dye removal using low cost adsorbents. Water Sci Technol 1997;36:189–96.

[34] Liu XD, Tokura S, Haruki M, Nishi N, Sakairi N. Surface modification of nonporous glass beads with chitosan and their adsorption property for transition metal ions. Carbohyd Polym 2002;49:103–8.

[35] Oshita K, Oshima M, Gao Y, Lee K-H, Motomizu S. Synthesis of novel chitosan resin derivatized with serine moiety for the column collection/concentration of uranium and the determination of uranium by ICP-MS. Anal Chim Acta 2003;480:239–49.

[36] Benesch J, Tengvall P. Blood protein adsorption onto chitosan. Biomaterials 2002;23:2561–8.

[37] Matsumoto M, Shimizu T, Kondo K. Selective adsorption

of glucose on novel chitosan gel modified by phenylboronate. Separ Purif Technol 2002;29:229–33.
[38] Strand SP, Vårum KM, Østgaard K. Interactions between chitosans and bacterial suspensions: adsorption and flocculation. Colloids and Surfaces B: Biointerfaces 2003;27:71–81.
[39] Huang C, Chung YC, Liou MR. Adsorption of Cu(II) and Ni(II) by palletized biopolymer. J Hazard Mater 1996;45:265–77.
[40] American Public Health Association/AMERICAN water Work Association/Water Environment Federation. Standard method for examination of water and wastewater, 20th ed. Method 2120E. Washington (DC); 1998.